

Chapter 17

Development of Eco-efficient Geopolymer Masonry for Sustainability



Radhakrishna and K. Venugopal

Abstract Geopolymer has been considered a popular alternative to traditional cement. Materials which are rich in silica and alumina can be used along with traditional aggregates to prepare geopolymer mortar and masonry units. This chapter deals with the development of geopolymer masonry units such as brick (GPB), solid block (GPSB) and hollow block (GPHB). All these products were tested for dimensionality, water absorption, strength, modulus of elasticity, etc. They possessed better properties compared to traditional masonry units. The same units were used for making masonry prisms, and wallets. The prisms and wallets were loaded with axial and eccentric loads and tested for compression. The modulus of elasticity was also determined along with the crack pattern. Results indicated that the prisms and wallets performed exceedingly well compared to the traditional masonry structures. Moreover, no traditional cement is required in any stage of construction. The traditional water curing and thermal input is avoided. Based on this study, geopolymer masonry units are strongly recommended for the structural masonry without compromising properties.

Keywords Geopolymer · Sustainability · Eco-efficient · Masonry · Masonry units · Brick · Block · Hollow block · Prism · Wallet

17.1 Introduction

Geopolymers are the innovative, low carbon, energy efficient and eco-friendly green material for the sustainable environment (Dao et al. 2019; Zuo and Ye 2021; Bhogayata et al. 2020; Verma and Dev 2021). It is formed by the reaction of solid alumino-silicates with high concentration alkaline hydroxide or silicate solution

Radhakrishna (✉)

Department of Civil Engineering, RV College of Engineering, Bengaluru, Affiliated to Visvesvaraya Technological University, Mysuru Road, Bengaluru, Karnataka, India
e-mail: radhakrishna@rvce.edu.in

K. Venugopal

Department of Civil Engineering, SEA College of Engineering, Bengaluru, Affiliated to Visvesvaraya Technological University, Bengaluru, Karnataka, India

(Ren and Zhang 2019). This network of alumina-silicate materials was entitled as “geopolymers” by a French Scientist Prof. Davidovits (Norton and Provis 2020). Construction industry being one of the largest contributors for carbon emissions, research on sustainable material like geopolymer composites has gained momentum (Rahman and Al-Ameri 2021). Geopolymer products can reduce the emission of green-house gases which are responsible for global warming unlike cement products. Geopolymer has already shifted from emerging technology to adopted structural material for various purposes. Even though pre-processing and procurement of raw material is tedious, it is expanding its application and adaptability to meet the market demands (Norton and Provis 2020). Geopolymers possess higher mechanical properties, bond strength, resistance to heat, chemicals, alkalis and reduces corrosion compared to OPC composites (Bhogayata et al. 2020; Sakthidoss and Senniappan 2020; Rehman and Sglavo 2020; Nuruddin et al. 2016). With the increase in awareness about environmental impact and sustainable products, Research and Development activities are focused towards replacement of eco-detrimental Cement products by eco-friendly Geopolymer Composites (Ridha et al. 2018). Geopolymers/Alkali activated products are the third generation materials after lime and cement, have proved their low Carbon emission over OPC products to carry forward a sustainable environment for the next generation (Sikandar et al. 2019).

Masonry is a systematic arrangement of masonry units for a specific purpose. Masonry units are made from clay, mortar, concrete, calcium silicate etc. Bricks, solid blocks and hollow blocks are popular among masonry units. Solid and hollow blocks are manufactured using traditional concrete. Blocks are relatively larger in size than brick. Blocks are normally used to construct partition and load bearing walls. Hollow concrete blocks have one or more hollow cavities. The cavities act as good thermal insulators. To construct the wall, bricks/blocks are placed one at a time and held together firmly with fresh mortar which are timely tested and used. Though traditional masonry units are popular, they are neither eco-friendly nor sustainable, as they consume cement or soil or heat energy. Geopolymers are relatively new material without any traditional cement. The binders for making geopolymers are Class F fly ash, GGBS or any material which are dominant in silica and alumina. Fly ash is a marginal material from thermal power plants. The health and ecological challenges of disposal of fly ash can be minimized by using this by-product as building material. The technology used in making geopolymer masonry is the same as traditional masonry units except in basic ingredients. The aggregates used are the same but instead of water, an alkaline solution made out of sodium silicate and sodium hydroxide is used to mix the ingredients. Geopolymer mortar can be effectively used to make sustainable bricks/blocks which can make effective structural masonry (Venugopal and Radhakrishna 2016a, b; Radhakrishna et al. 2015; Radhakrishna and Venugopal 2020).

17.2 Bricks and Blocks

Sodium hydroxide flakes were added to the water depending on the required concentration to make sodium hydroxide solution. After preparing the sodium hydroxide solution, it is allowed to cool and sodium silicate was added to the same mix in required proportion. The alkaline solution was prepared 24 h earlier to the casting of bricks/blocks. The alkaline solution of 8 molar concentrations was prepared.

The geopolymer bricks (GPB), geopolymer solid blocks (GPSB) and geopolymer hollow blocks (GPHB) were mechanically cast using Class F fly ash and GGBS as binders. Alkaline solution was used as fluid, M-sand as fine aggregates. The proportions of these materials used in casting are as follows.

- Binders—80% Class F fly ash, 20% GGBS
- Binder: aggregates—1:1
- Ratio of alkaline solution to binders—0.2

The casting of Geopolymer bricks and blocks was done mechanically in the casting yard of a brick factory. The binders and aggregates were first added to the mixer and dry mixed for 5 min before the addition of alkaline solution. GPB, GPSB and GPHB were cast in an 8 MPa compression machine; pan mixer and belt conveyor are as shown in Fig. 17.1. The schematic representation of the typical masonry units and dimensions are as shown in Fig. 17.2.

The bricks and blocks were cast, kept in ambient curing conditions at room temperature in open air without any water or external curing agents. The finished geopolymer bricks and blocks are shown in Fig. 17.3a–c.

17.2.1 Tests on Geopolymer Masonry Units

Following tests were conducted



Fig. 17.1 Casting process

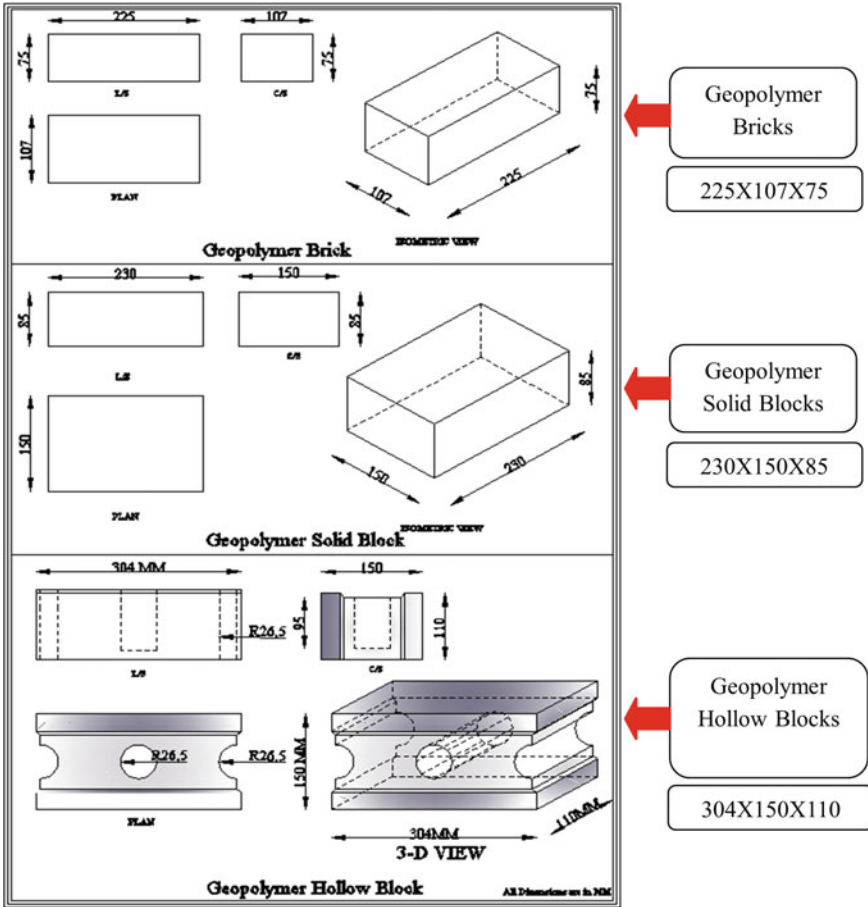


Fig. 17.2 Schematic representation showing the dimensions of the brick/block

- Dimensionality
- Density
- Water absorption
- Initial rate of water absorption
- Compressive strength
- Modulus of elasticity
- Microscopic Analysis
- X-ray Diffraction Analysis
- Flexural strength.



Fig. 17.3 a Geopolymer bricks, b geopolymer solid block, c geopolymer hollow block

17.2.1.1 Dimensionality Test

This test was conducted according to IS 1077-1992 (Standard 1997). The maximum deviation of the length of individual bricks should not be more than ± 5 mm, the maximum deviation of width and height should not be more than ± 3 mm. Twenty bricks were selected at random lined on a level floor successively in a straight line as shown in the Fig. 17.4a, b. The overall dimensions of the bricks were measured using steel tape.

The average variation of deviation of the length, breadth and depth of brick/blocks is shown in Table 17.1. It shows that the variation in the size of the bricks and block is

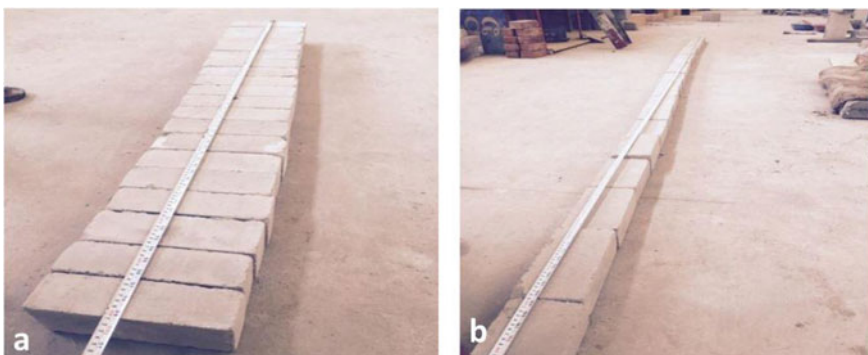


Fig. 17.4 Dimensionality test: a along breadth, b along length

Table 17.1 Results of dimensionality test

Brick/block	Dimensions measured along	Size (mm)	Measurements (mm)	Average measurements (mm)	Variation in measurements (mm)	IS 1077:1992
Geopolymer brick	Length (L)	225	4560	228.0	+3.0	±5
	Breadth (W)	107	2157	107.85	+0.85	±3
	Height (H)	75	1509	75.45	+0.45	±3
Geopolymer solid block	Length (L)	230	4614	230.70	+0.75	±5
	Breadth (W)	150	3012	150.60	+0.60	±3
	Height (H)	85	1724.4	86.24	+1.24	±3
Geopolymer hollow 'block	Length (L)	304	6103	305.15	+1.15	±5
	Breadth (W)	150	3015	150.75	+0.75	±3
	Height (H)	110	2221	111.05	+0.05	±3

Table 17.2 Results of density test

Type of block	Density (kg/m ³)	IS 2185:2008 (kg/m ³)
Geopolymer brick	1800	1800–2000
Geopolymer solid block	1810	
Geopolymer hollow block	1750	

within the range of codal limits. Bricks/blocks satisfied the specifications for length, width and height.

17.2.1.2 Density Test

This test was done as per IS 2185-2008 (Part 4). The findings are shown in Table 17.2. The density of geopolymer brick, solid block and hollow blocks are less comparable to the regular conventional blocks due to usage of the fly ash. The densities of the units are within the range of acceptable limits.

17.2.1.3 Water Absorption Test

The water absorption test was carried out according to IS 3495: 1992-Part 2. They fall in the category of up to class brick of strength 12.5 MPa as per code and it is represented in Table 17.3.

Table 17.3 Results of water absorption Test

Type of block	Water absorption (%)
Geopolymer brick	8.5
Geopolymer solid block	8.3
Geopolymer hollow block	9.1

Table 17.4 Results of initial rate of absorption test

Type of block	Initial rate of absorption IRA (kg/m ² /min)
Geopolymer brick (GPB)	3.0
Geopolymer solid block (GPSB)	2.7
Geopolymer hollow block (GPHB)	2.5

17.2.1.4 Initial Rate of Water Absorption (IRA) Test

This test was conducted according to ASTM C67-1299 (ASTM 2009). The results are indicated in Table 17.4. Initial rate of water absorption of GPB, GPSB and GPHB is less than the regular conventional blocks; these values are within codal limits.

17.2.1.5 Compressive Strength Test

This test was conducted according to IS 1077-1992 (Standard 1997). The compressive strength development of brick/blocks with age is represented in Fig. 17.5. IS 1077-1992 specifies minimum compressive strength of conventional bricks at 28 days as 3.5 MPa, whereas the compressive strength of the Geopolymer masonry units is

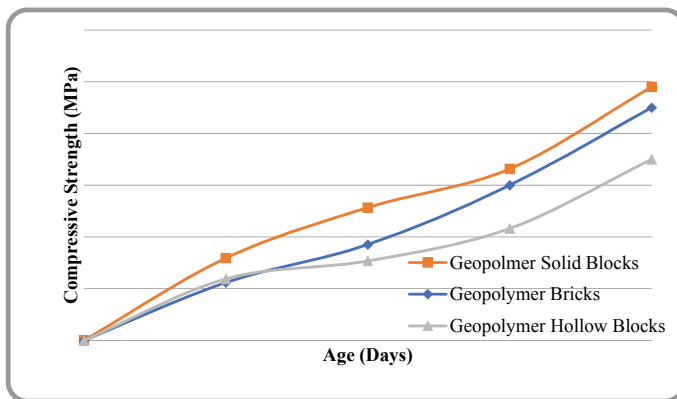


Fig. 17.5 Compression strength of bricks and blocks

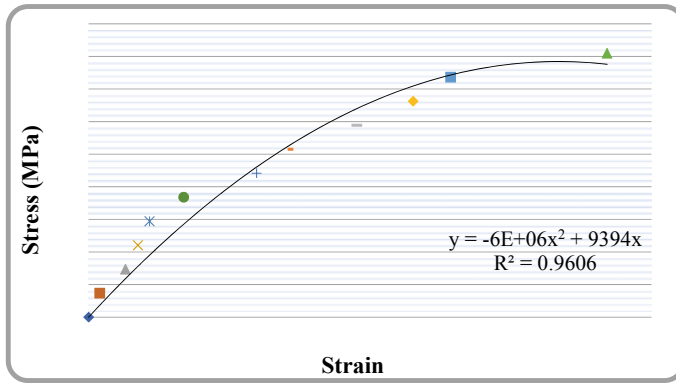


Fig. 17.6 Stress-strain curve for 8M NaOH bricks/blocks

more than the minimum strength and these were satisfied by the code provision. Also noted that the geopolymer brick and the solid blocks are having more strength compared to the geopolymer hollow blocks due to the voids or hollow portions of the blocks.

17.2.1.6 Modulus of Elasticity Test

The elastic modulus (E) is a very important characteristic in determining how the entire masonry will behave. It is particularly helpful for design calculations and assessment of deformation characteristics. Five specimens were tested to find modulus of elasticity. Initial tangent modulus of 8M NaOH bricks/blocks was found out to be 9394 MPa which is higher than that of traditional clay bricks manufactured in India (Rao 1986). A typical stress-strain curve for the geopolymer brick/block represented in Fig. 17.6.

17.2.1.7 Scanning Electron Microscope (SEM) Analysis

Microscopic image of 8M NaOH brick/blocks is as shown in Fig. 17.7. It indicates the presence of unreacted fly ash particles and aluminosilicate gel phases and the un-reacted fly ash particles of less than $10\ \mu\text{m}$ size. It is due to the use of low concentration of alkaline solution. The use of high molarity solution will develop higher strength.

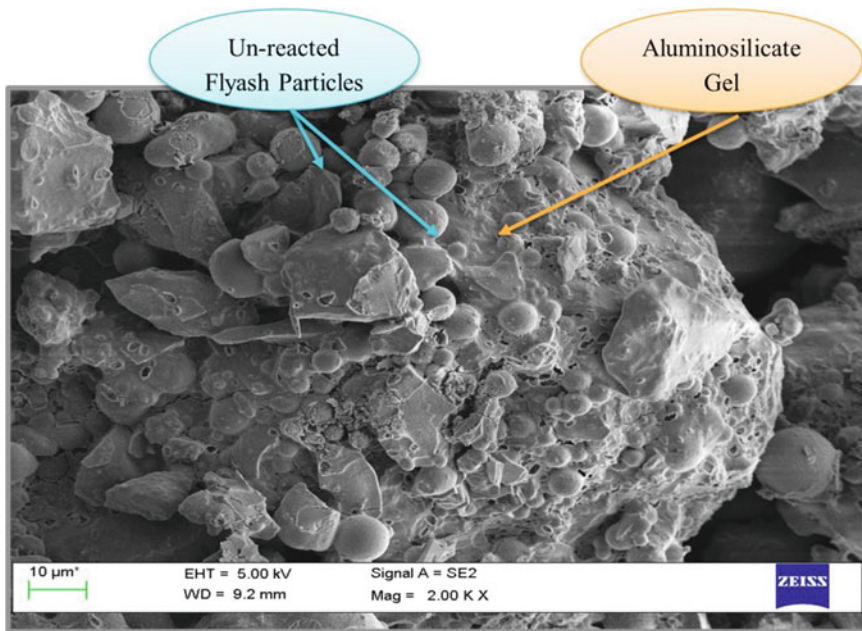


Fig. 17.7 Scanning electron microscope image of 8M NaOH brick

17.2.1.8 X-RAY Diffraction (XRD) Analysis

X-ray diffraction is a method used to obtain the internal lattice of crystalline materials and to obtain information on unit cell dimensions from the information generated by X-ray. XRD test on materials of 8M NaOH bricks/blocks was conducted. The X-ray diffractogram (XRD) is shown in Fig. 17.8. The diffractogram indicates the presence of crystalline phases of quartz and mullet. The base hump in the graph indicates the presence of amorphous silica or reactive silica. The corresponding material composition of the brick/blocks is shown in Table 17.5.

17.2.1.9 Flexural Strength

This test was conducted according to IS 4860-1968 as shown in Fig. 17.9. Flexural strength of the 8M NaOH Bricks and blocks are shown in Table 17.6. The flexural strength of the GPB at 28 days as per IS 4860-1968 is minimum of 10% that of the compressive strength. The flexural strength of GPB, GPSB and GPHB are 1.36, 1.55 and 1.79 MPa respectively. Flexural strength of geopolymer bricks/blocks is much higher than the regular conventional bricks and also noted that the flexural strength of the hollow block is much higher than that of the solid block and the brick because of the increase in thickness of the hollow blocks.

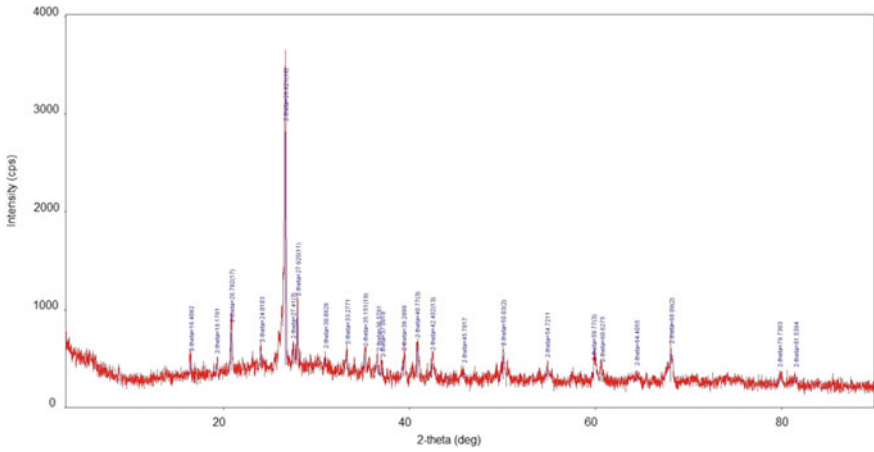


Fig. 17.8 X-ray diffraction results of 8M NaOH bricks/blocks

Table 17.5 Material composition of the brick/block

Phase name	Content (%)
Quartz	69.0
Mullite	12.2
Gossypol acetic acid	0.0
Vaterite	18.0

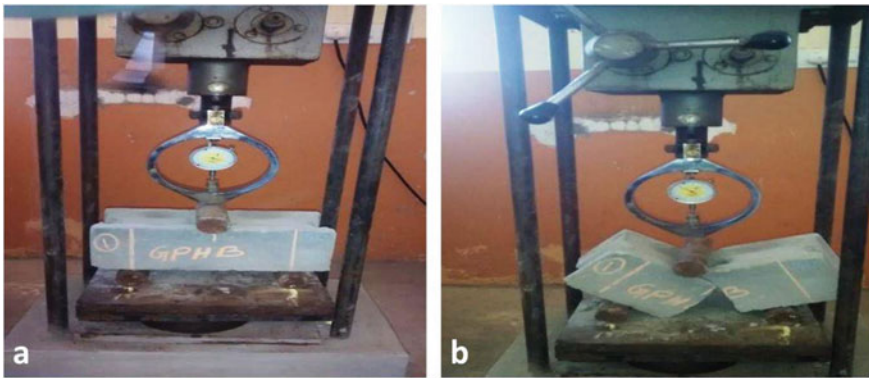


Fig. 17.9 Flexural strength test setup: **a** test setup, **b** failure pattern

Table 17.6 Results of flexural strength of the bricks/blocks

Type of block	Average flexural strength (MPa)
Geopolymer brick	1.36
Geopolymer solid block	1.55
Geopolymer hollow block	1.79

Cement mortar and geopolymer mortar was used for casting masonry prisms and wallettes. The mortars were cast as per the recommendations of IS 2250-1981. The binders and inert filler materials were first mixed dry till a homogenous mixture was obtained. The water/alkaline solution was added and mixed for 5–10 min to obtain the uniform mix of cement mortar/geopolymer mortar.

17.3 Geopolymer Masonry Prism

One of the major forces that masonry has to deal with is compression. Therefore, it is important to know the behavior of masonry in compression. Masonry efficiency in compression is an important parameter to determine the permissible stresses required for the design of masonry structures. Masonry efficiency was determined by a prism test as specified by IS 1905-1987. As per the code, the h/t ratio of the prism is to be in the range 2–5.

Stack bonded prisms are the prisms cast by keeping masonry units, one above the other with mortar placed in between them. Five brick thick stack bonded prisms were cast using 8M NaOH bricks and 12.5 mm cement mortar/Geopolymer mortar and the 4brick thick and 3 brick thick stack bonded prisms were cast using 8M NaOH bricks and 7.5, 10 and 12.5 mm cement mortar joints. Five-block, four-block and Three-block thick stack bonded solid and hollow block prisms were also cast using 8M NaOH blocks and 7.5, 10 and 12.5 mm cement mortar joints. The stack bonded prisms are as shown in Fig. 17.10.

Unrendered is the portion not covered by plaster or stucco for all faces. To study the effect of mortar joint thickness on masonry efficiency, stack bonded prisms were



Fig. 17.10 Stack bonded prisms



Fig. 17.11 Unrendered stack bonded prisms

cast using 8M NaOH bricks and 7.5, 10 and 12.5 mm cement mortar/Geopolymer mortar. The bricks were immersed in water before casting to ensure the saturated condition of the brick so that it will not absorb water from the mortar. The unrendered prisms are as shown in Fig. 17.11. Prisms which were cast using cement mortar were cured in water while the prisms cast using geopolymer mortar were kept in open air for curing. Prisms were cured for 28 days before the test.

17.3.1 Testing of Brick Prisms

The testing arrangements of brick prisms are shown in Fig. 17.12. Prisms were kept on the loading frame and leveled using the level tube. Steel plates were provided on top of the specimen to ensure uniform distribution of loads and also to act as filler materials. The centerline of the prisms was marked. Two metal studs were fixed on both the sides of the center line along the vertical direction. Then the displacement measuring device gauge was fixed on these studs. Loading was done at the rate of 350 kN/min by a hydraulic jack of 500 kN capacities. For axial loading, the jack was placed exactly in the center of the bearing surface of the prism and the eccentric loading; the jack is placed from the center from a distance of 1/6th from the center. Proving ring of 500 kN capacity was placed to measure load at regular intervals. Deformation was noted at regular intervals of loading until the failure of the specimen occurred. The compressive stress calculated as 0.25 times the compressive strength was compared with the values given in Table 21.8 of IS 1905-1987.

Fig. 17.12 Testing arrangement of stack bonded prisms



Variations of masonry efficiency in mortar joint thickness for prisms cast using cement mortar after applying the correction factor given in IS 1905-1987 are as shown in Table 17.7. Permissible stresses for masonry are based on the values of basic compressive stress. Basic compressive stress is given in the code IS 1905-1987

Table 17.7 Basic compressive stress of stack bonded geopolymer brick prisms

h/t ratio	Mortar joint thickness (mm)	Average Compressive strength (f'_m)	Basic compressive stress = $0.25 \times f'_m$
3.97	12.5	3.00	0.75
3.88	10.0	3.05	0.76
3.78	7.5	3.25	0.81
3.15	12.5	2.72	0.68
3.08	10.0	3.01	0.75
3.01	7.5	3.20	0.80
2.33	12.5	2.55	0.64
2.28	10.0	2.71	0.67
2.24	7.5	2.95	0.74

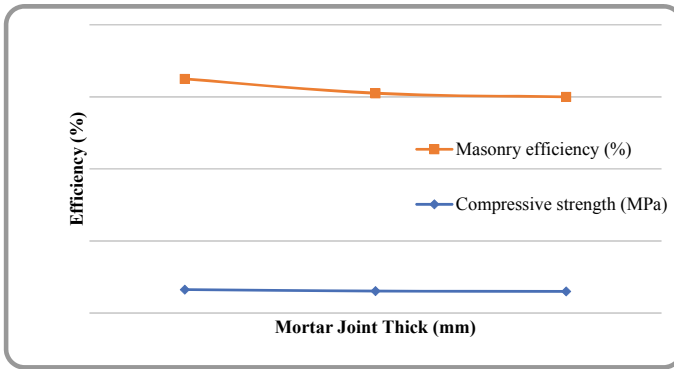


Fig. 17.13 Stack bonded 5 brick thick geopolymer prism with cement mortar joints

for burnt clay bricks. These values were compared with that of geopolymer bricks obtained from the prism test. Basic compressive stress for the geopolymer brick prisms is 10 MPa, the Crushing strength and M2 grade mortar as per Table 8 of the code after applying suitable corrections is 0.6 MPa. The basic compressive stress of prism test can be calculated as Basic Compressive stress = $0.25X f'_m$ Where f'_m is Compressive strength of prism

$$\text{Basic compressive stress} = 0.25 \times f'_m$$

It was noticed that the masonry efficiency of prisms cast using Geopolymer Bricks and cement mortar decreased with the increment in mortar joint thickness as shown in Fig. 17.13. Basic compressive stress by prism tests is given in Table 17.7. It was found that the basic compressive stress of all the prisms was greater than that given in Table 8 of the code IS 1905-1987.

Stress and strain were recorded at various intervals. The typical variation was plotted as shown in Fig. 17.14 after normalizing the values. Modulus of elasticity of the prisms increased slightly with the decrease in mortar joint thickness. Initial tangent modulus for prisms with 12.5 mm mortar thickness was 7005, 7111 MPa for prisms with 10 mm mortar thickness and 7314 MPa for prisms with 7.5 mm mortar thickness. There was no much difference in modulus of elasticity with various h/t ratios of the prisms. The variation of stress with strain is almost linear. The behavior is like typical burnt brick masonry prisms.

The vertical cracks and vertical splitting of narrow faces originated from the top of a brick. The cracks propagate further down. It also noticed that the bottom most brick was crushed to a considerable extent. Typical failure patterns of the prisms are as shown in Fig. 17.15a–d.

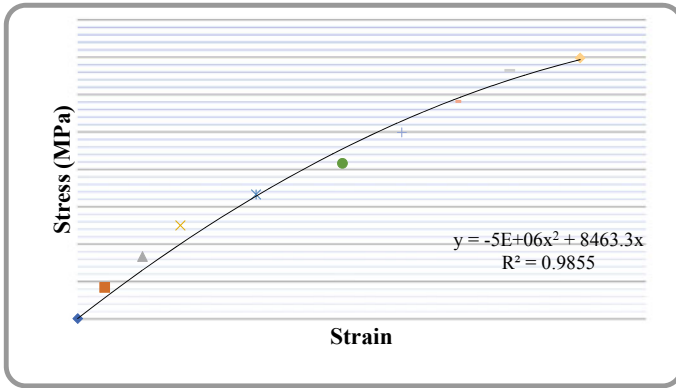


Fig. 17.14 Stress-strain curve for 10 mm thick joint cement mortar prism with $h/t = 3.08$



Fig. 17.15 Failure pattern of brick prisms

17.3.2 Testing of Geopolymer Solid Block Prisms

The test was done as per IS 1905-1987. The testing arrangements and method of rendered and unrendered solid block prisms are the same as geopolymer brick prisms and was discussed in the previous section. This study was made on geopolymer

solid block prisms cast using cement mortar. It was noticed that masonry efficiency, decreasing with the increment in mortar joint thickness as shown in Fig. 17.16. Basic compressive stress by prism tests is given in Table 17.8. It was found that the basic compressive stress of all the prisms was greater than that given in Table 8 of the code IS 1905-1987.

Stress and strain were recorded at various intervals. The typical variation was plotted as shown in Fig. 17.17 after normalizing the values. It was observed that the modulus of elasticity of the prisms increased slightly with the decrease in mortar joint thickness. Initial tangent modulus for prisms with 12.5 mm mortar thickness was 5831 and 6313 MPa for prisms with 10 mm mortar thickness and 8471 MPa for prisms with 7.5 mm mortar thickness. There was no much difference in modulus of elasticity with different h/t ratios of the prisms. The variation of stress-strain is almost linear. The behavior is like typical burnt brick masonry prisms.

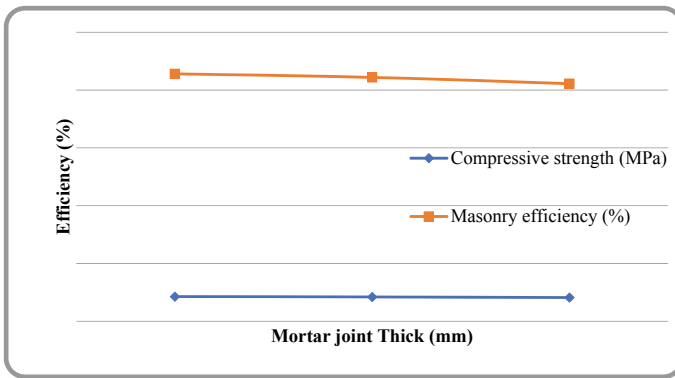


Fig. 17.16 Stack bonded 5 brick thick geopolymer solid block prism with cement mortar joints

Table 17.8 Basic compressive stress of prisms

Mortar joint thickness (mm)	h/t ratio	Average compressive strength (f'_m)	Basic compressive stress = $0.25 \times f'_m$
12.5	3.17	4.11	1.02
10.0	3.10	4.22	1.05
7.5	3.03	4.28	1.07
12.5	2.51	3.89	0.97
10.0	2.46	3.87	0.96
7.5	2.41	4.06	1.01
12.5	1.86	3.73	0.93
10.0	1.83	3.76	0.94
7.5	1.80	3.89	0.97

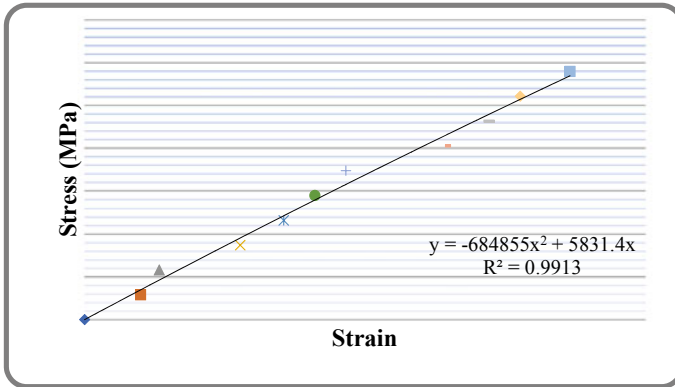


Fig. 17.17 normalized stress-strain curve for 12.5 mm thick joint cement mortar solid block prism with $h/t = 3.17$



Fig. 17.18 .

The vertical cracks are developed at the bottom of the block and it propagates till the top of the prisms and bottom most corners of the blocks where spalling had taken place. Typical failure patterns of the prisms are as shown in Fig. 17.18a, b.

17.4 Geopolymer Hollow Block Prisms (GPHB)

Casting procedure of 8M NaOH geopolymer hollow block prisms is the same as geopolymer brick prisms and this has been discussed in the previous section. Masonry efficiency is found as specified by IS 1905-1987. As per the code, the h/t ratio of the

Table 17.9 Mortar thicknesses and h/t ratios of stack bonded hollow block prisms

Mortar thickness (mm)	Prisms dimensions			h/t ratios
	H (mm)	B (mm)	T (mm)	
12.5	600	304	150	4.00
10	590	304	150	3.93
7.5	580	304	150	3.86
12.5	477.5	304	150	3.18
10	470	304	150	3.13
7.5	462.5	304	150	3.08
12.5	355	304	150	2.36
10	350	304	150	2.33
7.5	345	304	150	2.30

prism must be between 2 and 5. Rendered and unrendered stack bonded prisms were cast to determine their behavior under compression.

Five-brick, four-brick and three-brick thick stack bonded prisms were cast using 8M NaOH hollow block and 10 mm cement mortar joints. The prism dimensions, mortar thicknesses of the prisms and their corresponding h/t ratios are as shown in Table 17.9.

17.4.1 Testing of Geopolymer Hollow Block Prisms

The test was done as per IS 1905-1987. The testing arrangements and method of rendered and unrendered hollow block prisms are as same as geopolymer brick prisms and was discussed in the previous 5.1.2. Test setup is as shown in Fig. 17.19.

This study was made on geopolymer hollow block prisms cast using cement mortar. The influence of mortar joint thickness and effect on the unrendered masonry efficiency of stack bonded prisms is discussed in this section.

It was noticed that masonry efficiency, decreasing with the increment in mortar joint thickness as shown in Fig. 17.20. Basic compressive stress by prism tests is given in Table 17.10. It was found that the basic compressive stress of all the prisms was greater than that given in Table 8 of the code IS 1905-1987.

Stress and strain were recorded at various intervals. The typical variation was plotted as shown in Fig. 17.21 after normalizing the values. Modulus of elasticity of the prisms increased slightly with the decrease in mortar joint thickness. Initial tangent modulus for prisms with 12.5 mm mortar thickness was 5831 and 6313 MPa for prisms with 10 mm mortar thickness and 8471 MPa for prisms with 7.5 mm mortar thickness. There was no much difference in modulus of elasticity with different h/t ratios of the prisms.



Fig. 17.19 Testing arrangement of geopolymer hollow block stack bonded prisms

Fig. 17.20 Stack bonded 5 brick thick geopolymer hollow block prism with cement mortar joints

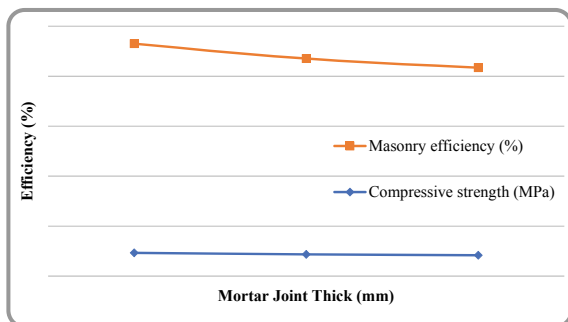
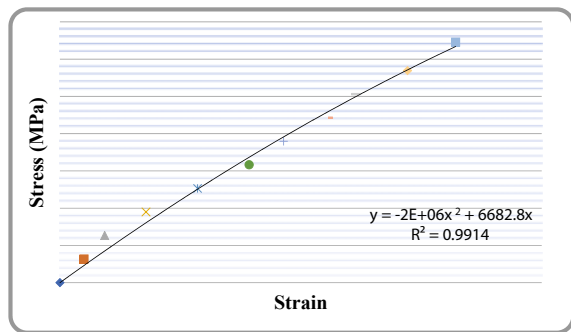


Table 17.10 Basic compressive stress of stack bonded prisms

h/t ratio	Mortar joint thickness (mm)	Average compressive strength (f'm)	Basic compressive stress = $0.25 \times f'm$
4.00	12.5	4.17	1.04
3.93	10.0	4.35	1.08
3.86	7.5	4.65	1.16
3.18	12.5	4.05	1.01
3.13	10.0	4.35	1.08
3.08	7.5	4.49	1.12
2.36	12.5	3.69	0.92
2.33	10.0	3.94	0.98
2.30	7.5	4.11	1.02

Fig. 17.21 Normalized stress-strain curve for 12.5 mm thick joint cement mortar hollow block prism with h/t = 4.0



The vertical cracks are developed at the center of the block and it continues till the bottom. Typical failure patterns of the prisms are as shown in Fig. 17.22a, b.

17.5 Wallettes

A brick/block wallette may be defined as the composite continuum of bricks/blocks and cement mortar joints. The details are as shown below.

- Bricks—8M NaOH bricks.
- Mortar—1:6 cement: River sand mortar of type M2 as per IS 1905-1987.
- Bed joint—10 mm thick mortar.
- Head joint—10 mm thick mortar.
- Concrete capping on top—75 mm thick.
- Wallette dimensions—(h × b × t) = 1105 × 1165 × 107 mm.
- h/t ratio = 10.32.

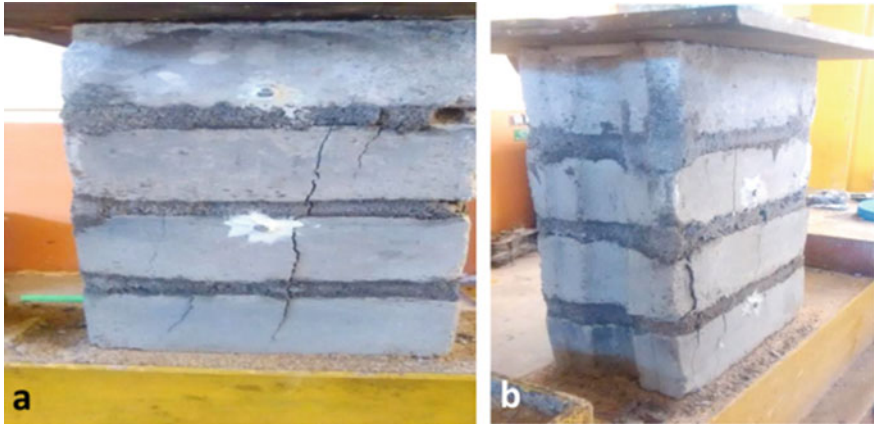


Fig. 17.22 Failure pattern for the unrendered geopolymer block prisms

The schematic representation of the typical wallette showing the dimensions is as shown in Fig. 17.23. The actual arrangements of units of geopolymer brick wallettes is shown in Fig. 17.24.

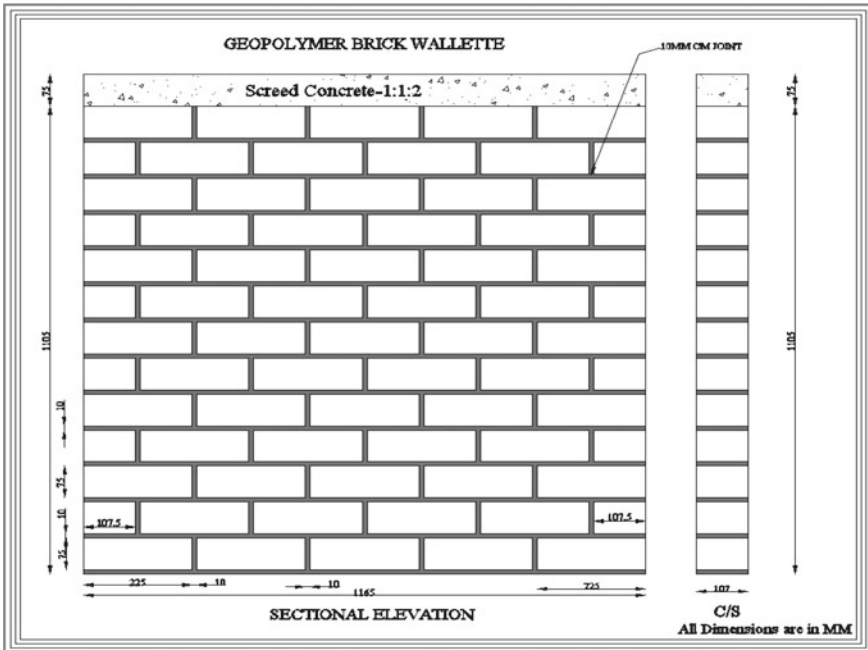


Fig. 17.23 Representation of typical geopolymer brick wallette



Fig. 17.24 Stretcher bonded geopolymer brick wallette kept for curing

The eccentricity adopted for wallette testing was the same as that adopted for English bonded prism, i.e., $e/d = 1/6$.

where e = eccentricity, d = bearing width = 107 mm.

From the above relation, eccentricity = $107/6$ which is approximately equal to 18 mm.

17.5.1 Testing of Geopolymer Bricks Wallettes

To make sure of uniform distribution of loading, 100 mm thick concrete capping was done on the brick wallettes. The load was applied at a uniform rate by a hydraulic jack of 1000 KN capacity. The load was distributed from the jack to the specimen by means of a ladder arrangement as shown in Fig. 17.25a. For axial loading, center of loading assemblage was placed on the center of bearing area of brick wallette. For eccentric loading, the center of the ladder arrangement was placed at a distance of 18 mm from the center of bearing surface of the wallette as shown in Fig. 17.25b.

The results of the axial loaded and eccentric loaded wallettes are given in Table 17.11. It was noticed that the masonry efficiency of eccentrically loaded wallette was 83% of that of an axially loaded wallette. Also it was observed that the compressive strength of the stretcher bonded wallette was 65% of the stack bonded prism of the same parameters.

Stress and strain were recorded at various intervals. The variation was plotted, and the initial tangent modulus of the wallette was higher in axial loading compared to eccentric loading. The initial tangent modulus of the wallette was 3528 and 2791 MPa for axial and eccentric loading respectively. Figure 17.26a and b show the stress-strain curve for axially loaded wallette and eccentrically loaded wallette respectively.



Fig. 17.25 Ladder arrangement for geopolymer brick wallette: **a** axial loaded brick wallette, **b** eccentric loaded

Table 17.11 Results of stretcher bonded geopolymer brick wallette

Type of loading	Wallette No	Load at initial crack (KN)	Failure load (KN)	Compressive strength (MPa)	Avg. compressive strength (MPa)
Axial loading	1	240.0	267.0	2.14	1.99
	2	200.5	229.8	1.84	
Eccentric loading	1	200.0	218.6	1.75	1.66
	2	170.0	197.2	1.58	

It was noticed that vertical cracks originated from the head joints on top of the wallette and it propagated, till three fourth of the height from top of the wallette. It also noticed that the width of the crack is increased up to 3 mm. Spalling of bed mortar joints have taken place in the eccentrically loaded wallettes. The failure patterns of axially loaded wallette and eccentrically loaded wallette are shown in Fig. 17.27a and b respectively. This behavior is similar to masonry wallettes.

17.5.2 Solid Block Wallettes

In this research, stretcher bonded solid block masonry wallettes were cast using GPS and cement mortar to check the effect of eccentric compression on masonry efficiency. Four wallettes were cast in the study, two wallettes each of axial compression and eccentric compression. The casting details are the same as geopolymer brick wallettes and as explained in the previous section and some of them are shown below.

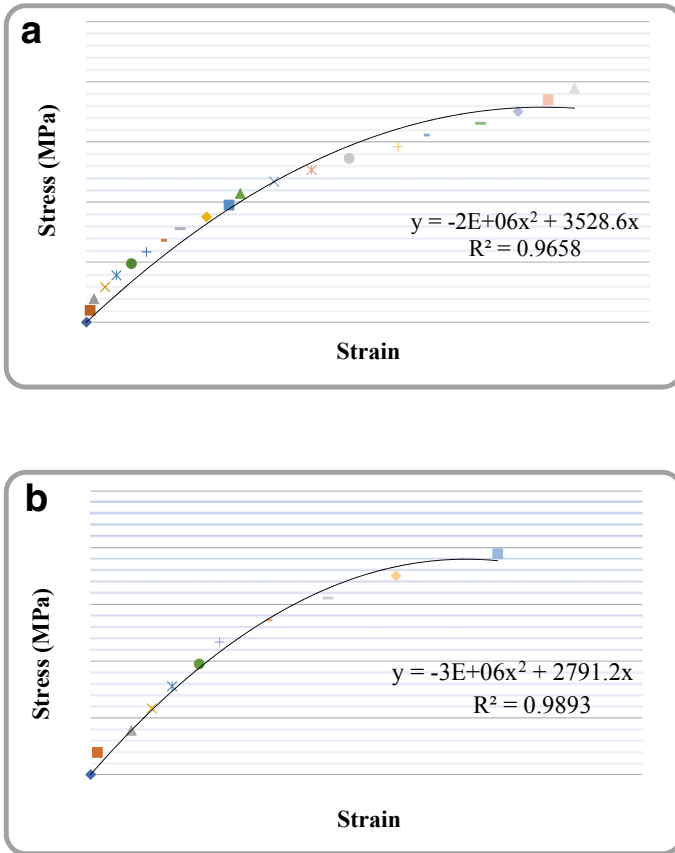


Fig. 17.26 **a** Stress-strain curve for axially loaded wallette. **b** Stress-strain curve for eccentrically loaded wallette

- Solid Block—8M NaOH blocks
- Wallette dimensions—(h × b × t) = 1034 × 1190 × 150 mm.
- h/t ratio = 6.90

The schematic representation of the typical solid block wallette showing the dimensions are as shown in Fig. 17.28a.

The wallettes cast was cured for 28 days after casting. Wallettes kept for curing are as shown in Fig. 17.28b.

The eccentricity adopted for wallette testing was the same as that adopted for English bonded prism, i.e., e/d = 1/6. Bearing width = 150 mm.

From the above relation, eccentricity = 150/6 which is approximately equal to 25 mm.

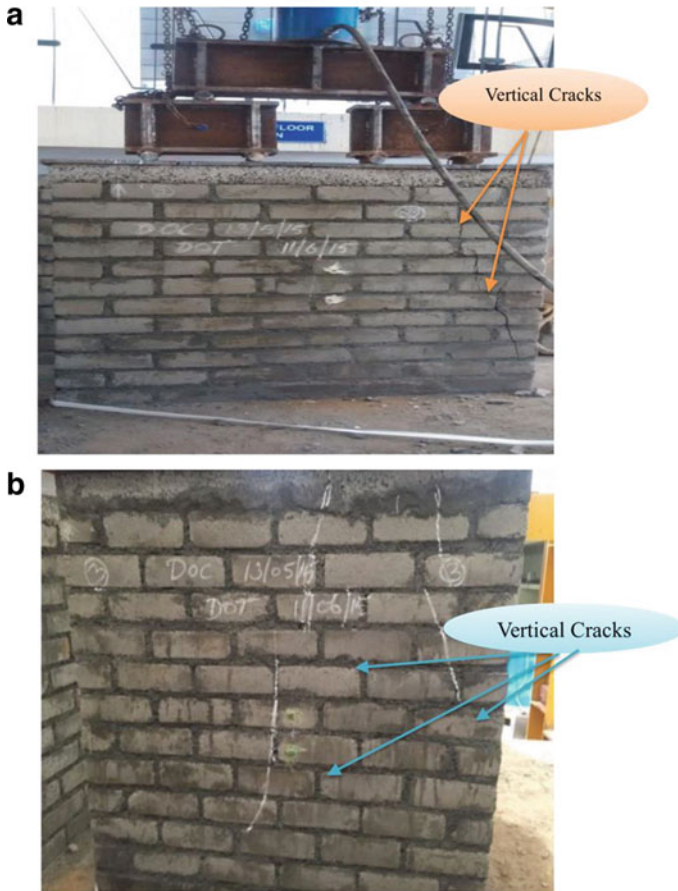


Fig. 17.27 a Failure pattern of axially loaded wallette, b Failure pattern of eccentrically loaded wallette

17.5.3 Testing of Geopolymer Soil Block Wallets

The testing arrangement of the solid block wallette was the same as that adopted for the geopolymer brick wallette and was discussed in the previous section. For eccentric loading, the center of the ladder arrangement was placed at a distance of 25 mm from the center of the bearing surface of the wallette.

The results of the axial loaded and eccentric loaded wallets are given in Table 17.12. It was noticed that the masonry efficiency of eccentrically loaded wallette was 90% of that of an axially loaded wallette. It was also noticed that the compressive strength of the stretcher bonded wallette was 50% of the stack bonded prism of the same parameters.

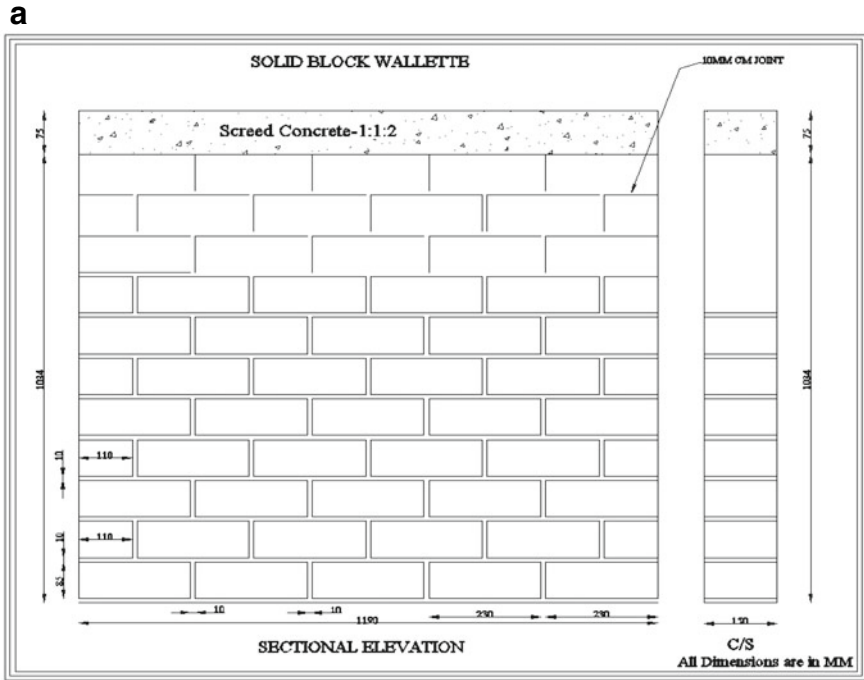


Fig. 17.28 a Schematic representation of typical geopolymer solid block wallette. b Stretcher bonded solid block wallette kept for curing

Table 17.12 Test results of stretcher bonded geopolymer solid block wallette

Type of loading	Wallette No	Load at initial crack (KN)	Failure load (KN)	Compressive strength (MPa)	Avg. compressive strength (MPa)
Axial loading	1	300	395	2.21	2.07
	2	275	345	1.93	
Eccentric loading	1	290	340	1.90	1.87
	2	265	330	1.84	

Stress and strain were recorded at various intervals. The variation was plotted, and the initial tangent modulus of the wallette was higher in axial loading compared to eccentric loading. The initial tangent modulus of the wallette was 3551 and 2787 MPa for axial and eccentric loading respectively. Normalized stress-strain curves for the same conditions are shown in Fig. 17.29a and b respectively.

It was noticed that vertical cracks were originated on top of the wallettes and it continued, till 2/3rd of the height from top. Spalling of bed mortar joints has taken place in the eccentrically loaded wallettes. The failure patterns of axially loaded wallette and eccentrically loaded wallette is shown in Fig. 17.30a and b respectively. This behavior is similar to any masonry wallettes.

17.5.4 Geopolymer Hollow Block Wallettes

In this research, stretcher bonded hollow block masonry wallettes were cast using GPHB and cement mortar to check the effect of eccentric compression on masonry efficiency. Four wallettes were cast in the study, two wallettes each of axial compression and eccentric compression. The casting details are the same as geopolymer brick wallettes and as explained in the previous section and some of them are shown below.

- Hollow Block—8M NaOH blocks
- Wallette dimensions—($h \times b \times t$) = 1080 mm \times 1246 mm \times 150 mm.
- h/t ratio = 7.2

The schematic representation of the typical hollow block wallette showing the dimensions is as shown in Fig. 17.31.

The geopolymer hollow block wallettes were cured for 28 days after casting. Wallettes kept for curing are as shown in Fig. 17.32a, b.

The eccentricity adopted for wallette testing was the same as that adopted for English bonded prism, i.e., $e/d = 1/6$.

where e = eccentricity, d = bearing width = 150 mm.

From the above relation, eccentricity = 150/6 which is approximately equal to 25 mm.

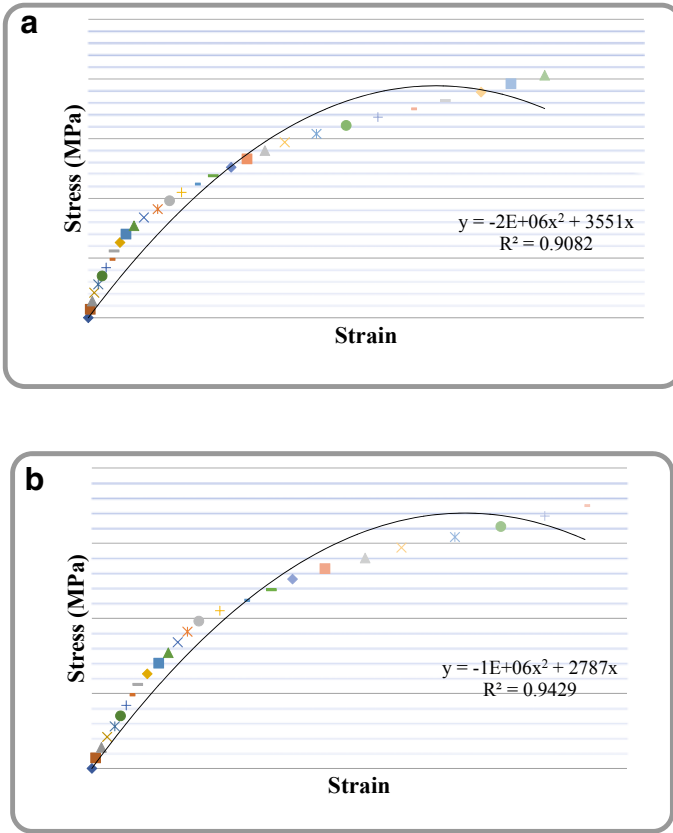


Fig. 17.29 **a** Stress-strain curve for axially loaded wallette. **b** Stress-strain curve for eccentrically loaded wallette

17.5.5 Testing of Geopolymer Hollow Block Wallettes

The testing arrangement for the hollow block wallette was the same as that adopted for the geopolymer brick wallette and was discussed in previous Sect. 5.7.1.1. The ladder arrangement for the geopolymer hollow block wallette is as shown in Fig. 17.33a. For axial loading, the center of loading assemblage was placed on the center of the bearing area of brick wallette. For eccentric loading, the center of the ladder arrangement was placed at a distance of 25 mm from the center of bearing surface of the wallette as shown in Fig. 17.33b.

The results of the axially loaded and eccentric loaded wallettes are given in Table 17.13. It was noticed that the masonry efficiency of eccentrically loaded wallette was 84% of that of an axially loaded wallette. It was noticed that the compressive strength of the stretcher bonded wallette was 53% of the stack bonded prism of the same parameters.

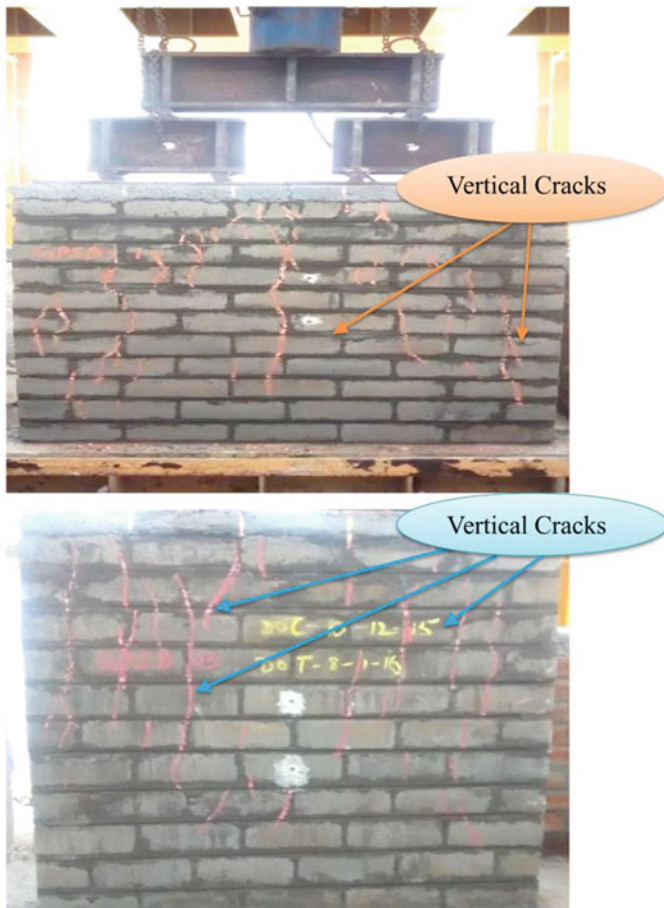


Fig. 17.30 Failure pattern: **a** axially loaded walette, **b** eccentrically loaded walette

Stress and strain were recorded at various intervals. The variation was plotted, and the initial tangent modulus of the walette was higher in axial loading than eccentric loading. The initial tangent modulus of the walette was 5834 and 2048 MPa for axial loading and eccentric loading respectively. Stress-strain curves for axially loaded walette and eccentrically loaded walette are shown in Fig. 17.34a and b respectively.

It was noticed that vertical cracks were originated at the top of the walleets and it continued, till 2/3rd of the height from the top and the crack width was increased up to 3 mm. It was observed that spalling of bed mortar joints has taken place in the eccentrically loaded walleets. The failure patterns of axially loaded walette and eccentrically loaded walette is shown in Fig. 17.35a and b respectively. This behavior is similar to any masonry walleets.

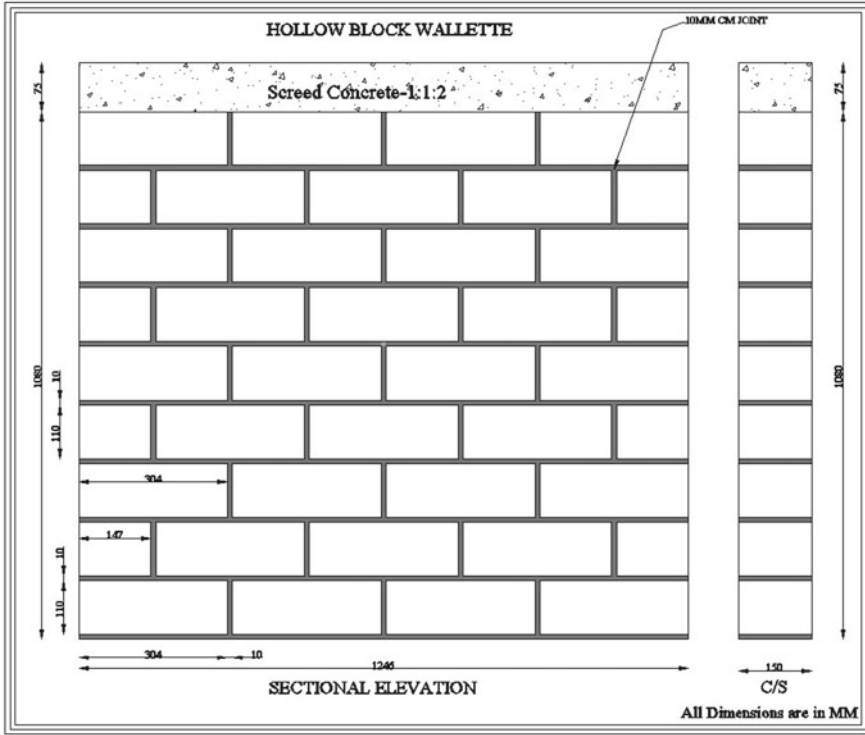


Fig. 17.31 Representation of typical geopolymer hollow block wallette



Fig. 17.32 Stretcher bonded hollow block wallette kept for curing: a front view, b top view



Fig. 17.33 Ladder arrangement for geopolymer hollow block wallette testing: **a** axial loaded wallette, **b** eccentric loaded

Table 17.13 Test results of stretcher bonded geopolymer hollow block wallettes

Type of loading	Wallette No	Load at initial crack (KN)	Failure load (KN)	Compressive strength (MPa)	Avg. compressive strength (MPa)
Axial loading	1	300	425	2.27	2.31
	2	380	442	2.36	
Eccentric loading	1	270	375	2.01	1.95
	2	245	355	1.89	

17.6 Conclusions

The following are the conclusions based on the discussion:

Fly ash and slag which are by-products of industry can be effectively used in making eco-efficient masonry units without compromising the properties. This addresses the challenges of disposing the by-products/marginal materials. The masonry units also depicted enhanced properties over conventional ones. They can be recommended to use in making structural masonry. Hence geopolymer masonry units proved to be eco-friendly and sustainable alternative building materials.

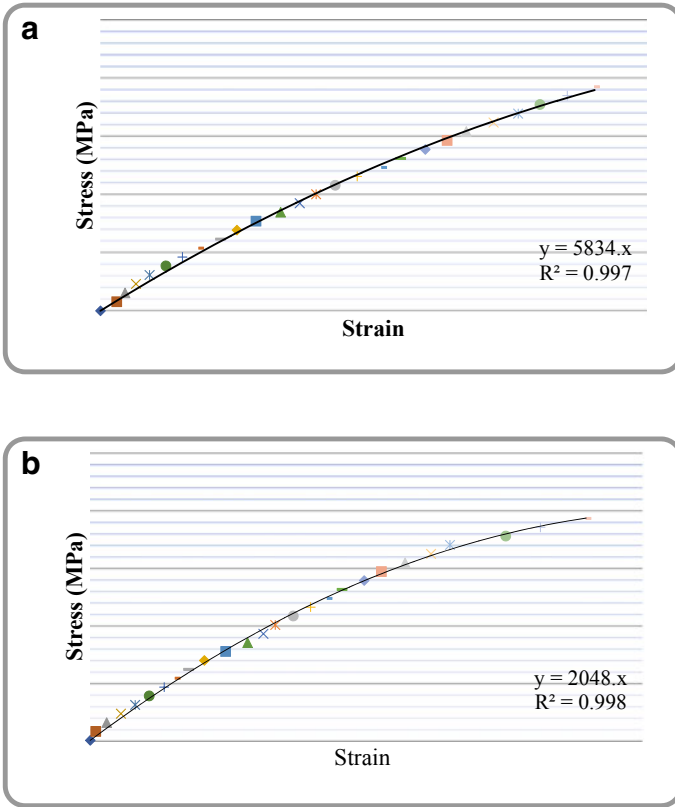


Fig. 17.34 a Stress-strain curve for axially loaded wallette. b Stress-strain curve for eccentrically loaded wallette

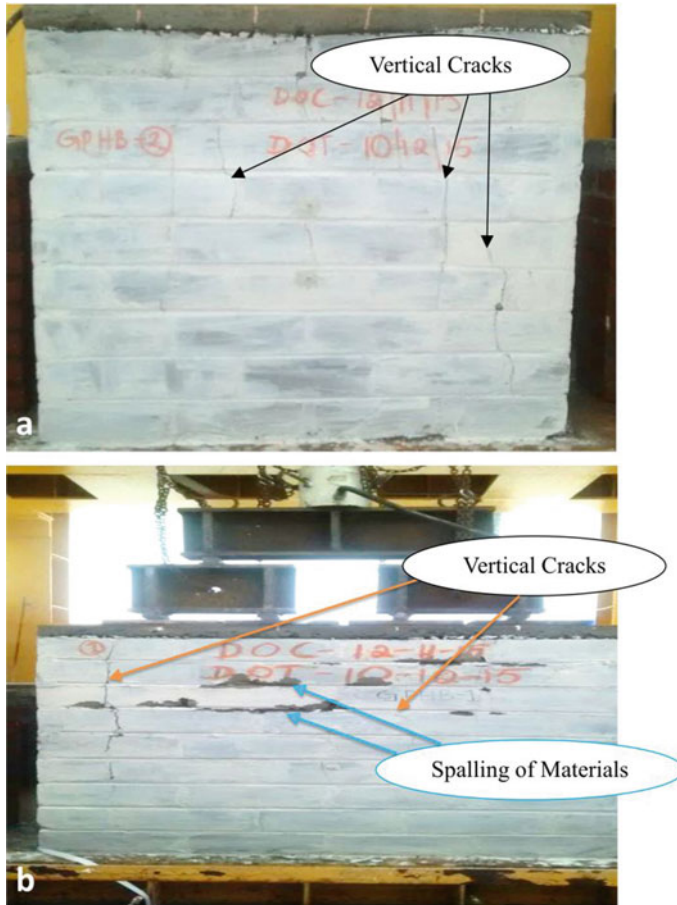


Fig. 17.35 Failure pattern: **a** axially loaded wallette, **b** eccentrically loaded wallette

References

ASTM (2009) ASTM C67-09. Standard test methods for sampling and testing brick and structural clay tile. American Society for Testing and Materials

Bhogayata A, Dave SV, Arora NK (2020) Utilization of expanded clay aggregates in sustainable lightweight geopolymer concrete. *J Mater Cycles Waste Manag* 22:1780–1792

Dao DV, Trinh SH, Ly HB, Pham BT (2019) Prediction of compressive strength of geopolymer concrete using entirely steel slag aggregates: novel hybrid artificial intelligence approaches. *Appl Sci* 9(6):1113

IS 1905-1987: Code of practice for structural use of unreinforced masonry. Bureau of Indian Standards, New Delhi

IS 2185 (Part 1)-2005: Concrete masonry units—Specifications Bureau of Indian Standards, New Delhi

IS 2250-1981: Code of practice for preparation and use of masonry mortars. Bureau of Indian Standards, New Delhi

- IS 3495 (parts 1 to 4)-1992: Methods of tests of burnt clay building bricks. Bureau of Indian Standards, New Delhi
- IS 4860-1968: Specification for acid resistant brick. Bureau of Indian Standards, New Delhi
- Norton MG, Provis JL (2020) 1000 at 1000: geopolymer technology—the current state of the art. *J Mater Sci* 55:13486–13489
- Nuruddin MF, Malkawi AB, Fauzi A, Mohammed BS, Almattarneh HM (2016) Geopolymer concrete for structural use: recent findings and limitations. In: IOP conference series: materials science and engineering, vol 133, No. 1. IOP Publishing, p 012021
- Radhakrishna VK, Sasalatti V, Venumadhav T (2015) Study of geopolymer masonry as sustainable building material. *J Environ Res Dev* 9(3A):925–932
- Venugopal K, Radhakrishna (2020) experimental study on behavior of geopolymer structural masonry. *Indian Concr J* 94(7):59–65
- Rahman SK, Al-Ameri R (2021) A newly developed self-compacting geopolymer concrete under ambient condition. *Constr Build Mater* 267:
- Rao NKS (1986) Structural masonry: properties and behavior. Department of Civil Engineering, IISc, Bangalore
- Rehman AU, Sglavo VM (2020) 3D printing of geopolymer-based concrete for building applications, concrete for building applications. *Rapid Prototyp J*
- Ren X, Zhang L (2019) Experimental study of geopolymer concrete produced from waste concrete. *J Mater Civ Eng* 31(7):04019114
- Ridha S, Abd Hamid AI, Setiawan RA, Shahari AR (2018) Influence of sulfuric and hydrochloric acid on the resistance of geopolymer cement with nano-silica additive for oil well cement application. *Int J Struct Integr*. <https://doi.org/10.1108/IJSI-11-2017-0066>
- Sakthidoss DD, Senniappan T (2020) A study on high strength geopolymer concrete with alumina-silica materials using manufacturing sand. *Silicon* 12:635–746
- Sikandar MA, Jo BW, Baloch Z, Khan MA (2019) Properties of chemically synthesized nano-geopolymer cement based self-compacting geopolymer concrete (SCGC). *J Wuhan Univ Technol Mater Sci Ed* 34(1):98–106
- Standard I (1997) IS 1077: 1992, Common burnt clay building bricks—specifications. Bureau of Indian Standards, New Delhi
- Venugopal K, Radhakrishna (2016a) Structural behavior of geopolymer masonry. *Indian J Sci Technol* 9(25):12–26
- Venugopal K, Radhakrishna (2016b) Sustainable units for structural masonry. *Indian J Sci Technol* 9(25):1–7
- Verma M, Dev N (2021) Effect of SNF-based superplasticizer on physical, mechanical and thermal properties of the geopolymer concrete. *Silicon* 1–11
- Zuo Y, Ye G (2021) GeoMicro 3D: A novel numerical model for stimulating the reaction process and microstructure formation of alkali activated slag. *Cem Concr Res* 141: